VOL. 11, NO. 16, AUGUST 2016 ISSN 1819-6608
ARPN Journal of Engineering and Applied Sciences


www.arpnjournals.com

EFFECT OF SYMMETRICAL COMPOUND-ANGLE IN COMBINED-HOLE FILM COOLING

Haswira Hassan and Kamil Abdullah
Center for Energy and Industrial Environmental Studies, Faculty of Mechanical and Manufacturing Engineering, Universiti Tun Hussein Onn Malaysia, Parit Raja, Johor, Malaysia
E-Mail: mkamil@uthm.edu.my

ABSTRACT

Due to high turbine inlet temperatures in modern gas turbines, film cooling technique was used to provide thermal protection for turbine components from being damaged by hot combustion gases. Combining two round-hole of film cooling is a better way to enhance the film cooling effectiveness. In the present work, a group of simulations consists of 27 cases using combined-hole unit with opposite compound-angle were carried out. The objective of this work is to find a good arrangement of combined-hole film cooling which produce better film cooling effectiveness. Effect of different blowing ratio, M with combination of different distance between two holes in mainstream direction, LoD, and compound-angle, γ_1 / γ_2 of film cooling hole were considered. As observed, lateral coverage was spread wider as the compound-angle and blowing ratio increase. While increasing LoD produces an insignificant results. However, increasing blowing ratio also resulting drastic decrease of film cooling effectiveness at further downstream. In the present study, area average film cooling effectiveness were determined to evaluate the general film cooling effect of different arrangements. Based on the area coverage, M = 1.5 shows an uncertain results for all arrangements. An early separation, spread and lift-off cause the different results at higher blowing ratio. The combination of the lateral distance of the two holes with their compound-angles for the highest film cooling effectiveness is different at different blowing ratios.

Keyword: film cooling, double-jet, combined-hole, compound-angle, film cooling effectiveness.

INTRODUCTION

The inlet temperature of a modern gas turbine had been raised year by year to improve the output power and thermal efficiency. But, the temperature supplied become higher than the melting point of the components material and able to compromise the durability of the components particularly the turbine blades. Therefore, enhancements of thermal protection on critical surfaces are required to ensure reliability of the turbine components. Film cooling method was applied as external protection to the components surfaces. The compressor bleed air was ejected through small holes on the blade body to provide cover to the blade surface by performing a thin layer of cooled air. While ensuring lower temperature and heat transfer on the turbine components, the thin layer also prevent direct contact between the hot gas and the surface of the components. Geometrical and flow parameters are some factors influence the performance of film cooling hole. Therefore, a good match between geometrical and flow parameters will produce great performance of film cooling.

LITERATURE REVIEW

From the beginning of this research field, cylindrical or single hole has been introduced as film cooling hole because it is simple and easy to fabricate. In 1971, Goldstein [1] as a pioneer in film cooling field presented a basic understanding of film cooling. In 1974, Goldstein *et al.* [2] study the effects of discrete holes angled at 35^o to the mainstream flow direction. By changing the blowing ratio, researchers analyzes that higher blowing ratio will significantly affect the performance of the film cooling. Higher blowing ratio will cause cooling gas separation from blade surface and produces a lift-off effects at downstream. Mainstream gas will flow beneath the cooling gas and pushed away the cooling gas from the blade surface. In 1996, Philllip M. Ligrani and Joon Sik Lee [3] doing experimental study of single hole film cooling with compound-angle. Follow by K. T. McGovern and J. H. Leylek [4] in 2000, they also had studied the cylindrical hole with various compound-angle injection. From both studies, an improved lateral spreading of the cooling gas was formed but, it was turns into one side. The counter-rotating vortex also becomes an asymmetrical with increasing of the compound-angle and fundamentally alters the interaction of the cooling gas and mainstream flow. To overcome the asymmetrical counter-rotating vortex and form anti-kidney vortex, researchers combined two cylindrical hole with opposite compound angle and named as combined-hole or double-jet film cooling hole. In 2007, Kusterer *et al.* [5] had reported that double-hole arrangement created an anti-kidney vortex while keep the cooling air covering the wall and distributed laterally. Besides that, in 2009, Kusterer *et al.* [6] also varied the flow parameter to simulate the combined-hole film cooling arrangement. In addition, Han *et al.* [7] in 2012 simulate variation geometrical parameter of combined-hole arrangement. Based on both studies, the suitable combination between geometrical parameter of combined-hole unit with flow parameter will produce better results and high film cooling performances.

METHODOLOGY

Computational domain

The basic configuration of the simulation consists of two main sections; mainstream and cooling gas duct embedded with combined-hole film cooling. Figure-1 shows details of the computational domain from top and side view. Figure-2 illustrated the details on the hole geometry. Mainstream direction was set along x-axis and the value of D was based on hole diameter, D equal to 3mm. The inclination angle, α was set as 30° in mainstream direction and pitch distance is equal to 5D. LoD and γ_1 / γ_2 were varied at three different value; 2.5D, 3.0D, 3.5D and -30º / 30º, -45º / 45º and -60º / 60º. As illustrated, the origin lies in the middle between two centers of combined-hole. Figure-3 shows the results for mesh dependency test conducted for the case of LoD = 3.0D and γ_1 / γ_2 = -45º / 45º at M = 0.5. Based on the mesh dependency test which involved the use of hybrid mesh, the total number of mesh elements used for each case is approximately 8.2 million.

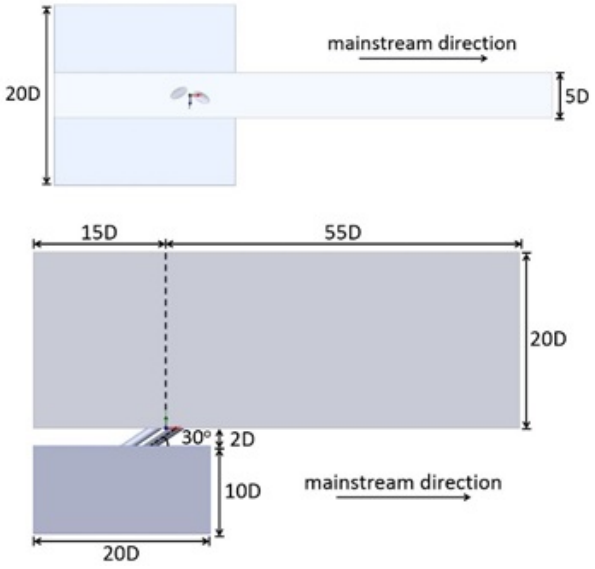

Figure-1. Details on computational domain.

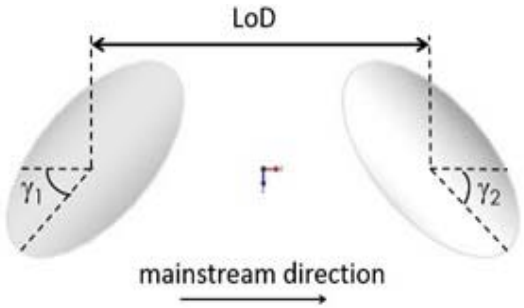

Figure-2. Details on hole geometry.

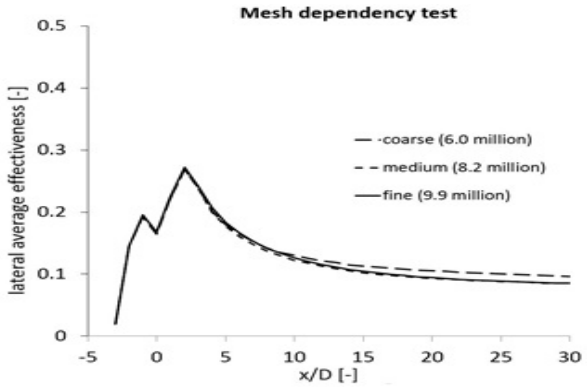

Figure-3. Mesh dependency test.

Numerical setup

The present study was carried out using ANSYS CFX software involving steady state Reynolds Average Navier Stokes (RANS) analysis with the employment of Shear Stress Transport (SST) turbulence model. The boundary and flow conditions applied in the present study are similar to the work of Han *et al.* [8] as shown in Figure-4 and Table-1. The mass flow rate of the cooling gas for the combined-hole have been determined with the assumption that both cooling holes are operating at the same blowing ratio and the sum of the required mass flow rate of each hole has been applied at the cooling gas inlet of the computational domain.

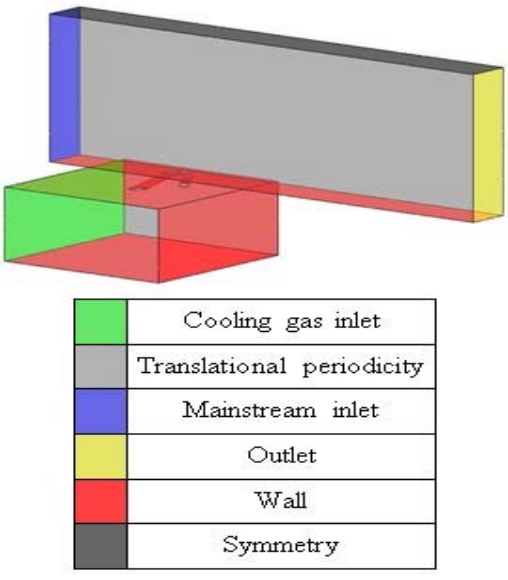

Figure-4. Boundary conditions.

Table-1. Flow conditions.

LoD	2.5D	3.0D	3.5D
γ_1 / γ_2	±30º	±45º	±60º

Validation

The numerical results of combined-hole film cooling effectiveness were validated with the experimental results of previous research reported by Han *et al*. [7]. Figure-5 shows the comparison of lateral average effectiveness results for experimental validation. The conditions of both cases were same as LoD = 3.0D and γ_1 / γ_2 = ±45º with M = 0.5. The numerical result is in agreement with the experimental result at near hole region and further downstream.

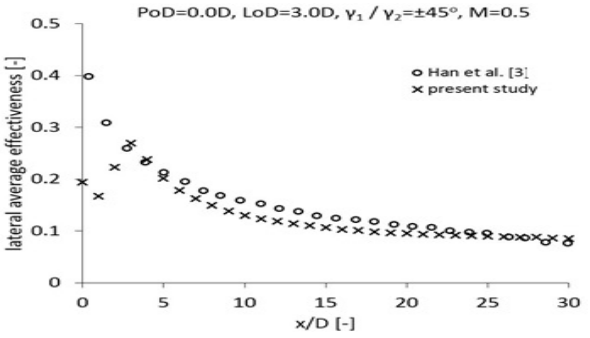

Figure-5. Experimental validation.

Performance indicator

$$\text{Film cooling effectiveness (fce)} = \frac{T_\infty - T_{aw}}{T_\infty - T_c}$$

T_∞ = Mainstream gas temperature
T_{aw} = Adiabatic wall temperature
T_c = Cooling gas temperature

RESULTS AND DISCUSSION

Film cooling effectiveness

Figure-6 show the film cooling effectiveness distributions for all considered arrangements. At low blowing ratio, significant change were not observed. Even LoD and γ_1 / γ_2 changed, film cooling effectiveness were not spreading laterally. Related with laterally average effectiveness graph in Figure-7, it shows same pattern of graph were produced for all arrangements with low laterally average effectiveness.

In Figure-8, wide coverage of film cooling effectiveness was observed at all arrangements. As illustrated, high film cooling effectiveness were produced as γ_1 / γ_2 increase. Increasing LoD shows a better results as shown in quantitative measured, Figure-9. Significant change can be observed as LoD increase with γ_1 / γ_2 = -30º / 30º. When γ_1 / γ_2 = -45º / 45º, change of LoD shows some improvements at halfway of mainstream direction but, going to have similar point further downstream. As γ_1 / γ_2 increase to -60º / 60º, it have same improvements as γ_1 / γ_2 = -45º / 45º but, LoD = 3.5D start to switch with lower LoD and have lower effectiveness further downstream compare to LoD = 2.5D and LoD = 3.0D.

When M = 1.5, a better lateral spread was observed but, early dissipation and low effectiveness region also developed downstream. In Figure-11, same pattern of graphs were shown. Graph γ_1 / γ_2 = -45º / 45º and γ_1 / γ_2 = -60º / 60º have high film cooling effectiveness at near hole region but tend to decrease at downstream, lower than γ_1 / γ_2 = -30º / 30º cases. Different with others blowing ratio, increasing in LoD for M = 1.5 shows uncertain results. It will discuss in next section, with explanation of area average effectiveness.

From overall observation of film cooling effectiveness, the lateral coverage of film cooling can be observed to increase as the compound-angle increase. Larger compound-angle lead the cooling gas to expand wider. For the small value of LoD, film cooling had insignificant impact. But, when the high LoD applied, the weakness of downstream hole as an obstacle for the cooling gas from upstream hole were reduced. The cooling gas from the upstream hole will move wider and directly penetrate into the mainstream without entering and combining with the flow come out from downstream hole.

Varied the flow parameter; blowing ratio also enhanced the film cooling effectiveness in lateral direction. Because of high momentum produced by high blowing ratio, the cooling gas was dissipated and decay faster when cooling gas penetrated with the mainstream flow. Therefore, low film cooling effectiveness region was produced faster as shown in Figure-10.

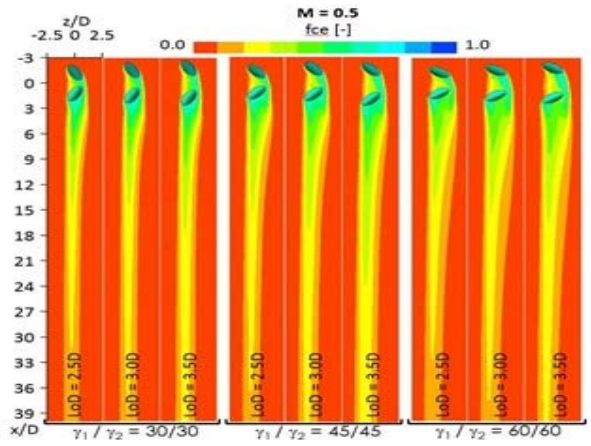

Figure-6. Film cooling effectiveness distributions at M = 0.5.

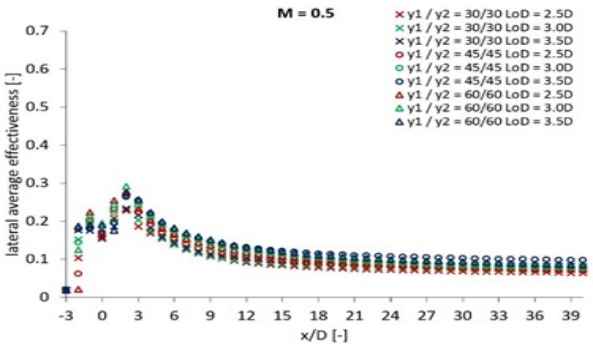

Figure-7. Lateral average effectiveness at M = 0.5.

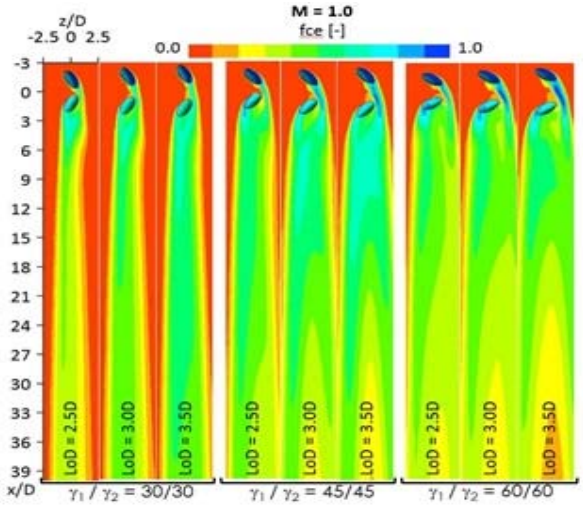

Figure-8. Film cooling effectiveness distributions at M =1.0.

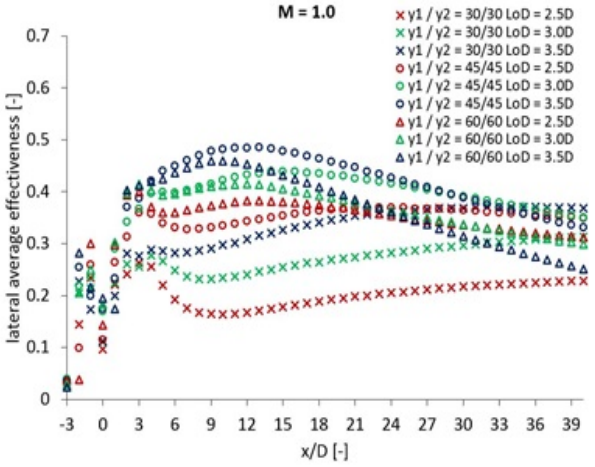

Figure-9. Lateral average effectiveness at M = 1.0.

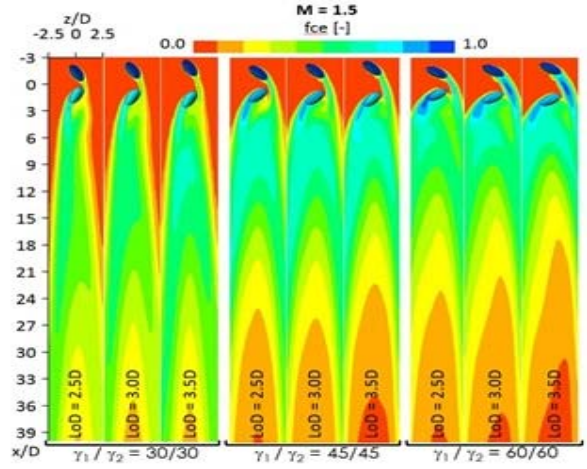

Figure-10. Film cooling effectiveness distributions at M = 1.5.

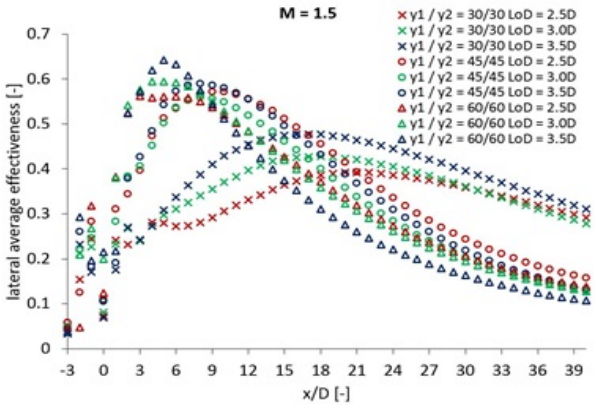

Figure-11. Lateral average effectiveness at M = 1.5.

Area average film cooling effectiveness

Figure-12 presented the results for area average film cooling effectiveness to evaluate the general film cooling effect of different arrangements. The width of the area is the pitch of combined-hole unit, 5D and the length was measured from origin to x/D = 40D. At lower blowing ratio, slight improvement showed as the LoD increase at all arrangements of compound-angle. The same pattern of improvement also can be observe at M = 1.0. At high blowing ratio, uncertain result were produced same as graph shown in Figure-11. Result for γ_1 / γ_2 = -30º / 30º increase as the LoD increase followed the increasing pattern at other blowing ratio. For γ_1 / γ_2 = -45º / 45º, LoD = 3.5D had low area average effectiveness compared to the low LoD of the same compound-angle while for γ_1 / γ_2 = -60º / 60º, the results were declined as the LoD increase.

Based on the uncertain results in Figure-11 and 12, the temperature contour on XY plane at several locations of x/D were shown for M = 1.5. Figure-13 shows the temperature contour for γ_1 / γ_2 = -30º / 30º cases at M = 1.5. Starting from x/D = 9, the cooling gas for LoD = 2.5D and LoD = 3.0D had 0.5 of effectiveness contour covering the wall. Compared to LoD = 3.5D, the effectiveness contour was 0.6 and still covering the wall until x/D = 12 Therefore, LoD = 3.5D shows a better cooling coverage for γ_1 / γ_2 = -30º / 30º results because of film cooling covered than the others.

Figure-14 shown the temperature contour for γ_1 / γ_2 = -45º / 45º cases at M = 1.5. Related with Figure-11, LoD = 3.5D with γ_1 / γ_2 = -45º / 45º shows higher lateral average effectiveness at x/D = 8 compared to the other LoD. But, starting from x/D = 10, the lateral average effectiveness of LoD = 3.5D start to shift and decrease below the other LoD. As illustrated in Figure-14, the spread of the flow for three different LoD almost the same at x/D = 9 and x/D = 10. But, starting from x/D = 11, LoD = 3.5D showed a wider spread of the flow and continues to expand as shown at x/D = 12. Effectiveness of 0.4 was observed covering at z/D = 0 for LoD = 3.5D and caused low area average effectiveness compared to the other LoD as indicated in Figure-12.

For γ_1 / γ_2 = -60º / 60º cases, the effectiveness coverage on the wall is low when LoD high. The spread of the flow also become wider at further downstream. As illustrated in Figure-15, low effectiveness contour, 0.2 was covered at z/D = 0.5 of LoD = 3.5D case on x/D = 12 compared to the lower LoD. Because of that situation, it produced the area average effectiveness as Figure-12; declined as the LoD increased at γ_1 / γ_2 = -60º / 60º case.

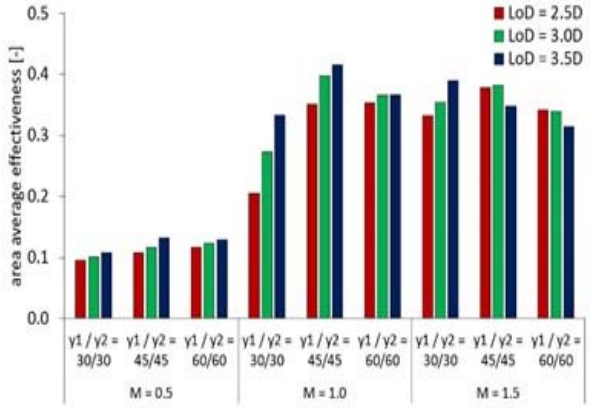

Figure-12. Area average film cooling effectiveness.

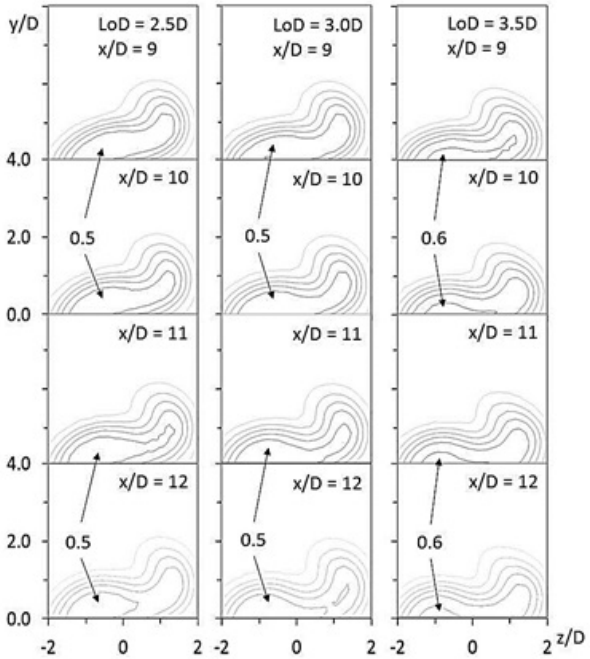

Figure-13. Temperature contour for γ_1 / γ_2 = -30º / 30º, M = 1.5.

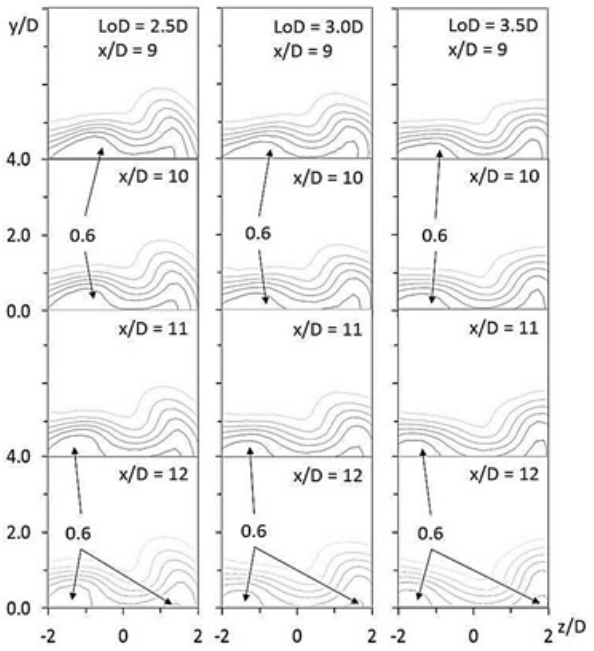

Figure-14. Temperature contour for γ_1 / γ_2 = -45º / 45º, M = 1.5.

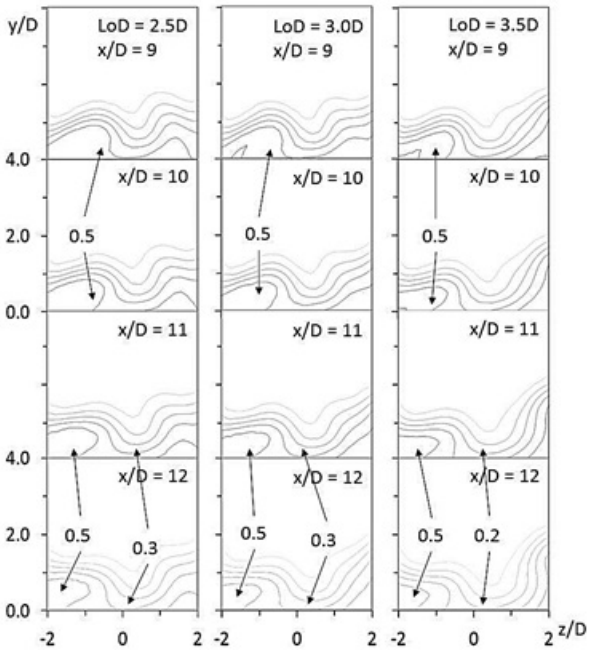

Figure-15. Temperature contour for γ_1 / γ_2 = -60º / 60º, M = 1.5.

CONCLUSIONS

A batch of simulation focused on the arrangements of combined-hole film cooling system had been carried out using steady state Reynolds Averaged Navier Stokes (RANS) method of ANSYS CFX, with Reynolds number, Re = 4200 at blowing ratios, M = 0.5,

1.0, and 1.5. Nine different computational models with combination of three different compound-angle and LoD have been considered in the present study. The conclusion for present study are as follow:

- Minimal impact were observed as LoD increased while increasing compound-angle improved lateral coverage of cooling gas.
- Significant effect were produced as blowing ratio increased.
- The lateral average effectiveness showed same pattern of results at different blowing ratio. High effectiveness occur at near hole region and descend further downstream.
- The optimal arrangement of combined-hole unit were made based on the area average effectiveness bar chart. At M = 0.5, the arrangement with γ_1 / γ_2 = -45º / 45º and LoD = 3.5D shows the higher area average effectiveness. For M = 1.0 and M = 1.5, the best combination of γ_1 / γ_2 and LoD are -45º / 45º, 3.5D and -30º / 30º, 3.5D.

REFERENCES

[1] R. J. Goldstein, Film cooling, (Adv. Heat Transf., vol. 7), pp. 321–379, 1971.

[2] R. J. Goldstein and E. R. G. Eckert, Effects Of Hole Geometry And Density On Three-Dimensional Film Cooling P & G, 1974.

[3] P. M. L. Grani, Film Cooling from a Single Row of Compound Angle Holes at High Blowing Ratios, pp. 259–267, 1996.

[4] K. T. Mcgovern and J. H. Leylek, A Detailed Analysis of Film Cooling Physics : Part II — Compound-Angle Injection With Cylindrical Holes, January 2000.

[5] K. Kusterer, D. Bohn, T. Sugimoto, and R. Tanaka, Double-Jet Ejection of Cooling Air for Improved Film Cooling, J. Turbomach., p. 809, 2007.

[6] K. Kusterer, A. Elyas, D. Bohn, T. Sugimoto, R. Tanaka, and M. Kazari, A Parametric Study on the Influence of the Lateral Ejection Angle of Double-Jet Holes on the Film Cooling Effectiveness for High Blowing Ratios, pp. 199–211, 2009.

[7] C. Han, J. Ren, and H. Jiang, Multi-Parameter Influence On Combined-Hole Film Cooling System, Int. J. Heat Mass Transf., pp. 4232–4240, 2012.

[8] C. Han, Z. Chi, J. Ren, and H. Jiang, Optimal Arrangement of Combined-Hole For Improving Film Cooling Effectiveness, pp. 1–11, 2013.